ADVANCING EARTH AND SPACE SCIENCE

Geophysical Research Letters

RESEARCH LETTER

10.1029/2021GL097413

Antarctic Sea Ice Projections Constrained by Historical Ice Cover and Future Global Temperature Change

C. R. Holmes[1], T. J. Bracegirdle[1], and P. R. Holland[1]

[1]British Antarctic Survey, Cambridge, UK

Key Points:

- We compare Coupled Model Intercomparison Project (CMIP), phase 5 and the CMIP, phase 6 (CMIP6) projections of Antarctic sea ice loss, assessing drivers of uncertainty and the robustness of projections
- Under strong forcing, CMIP6 models lose most Antarctic summer sea ice by 2100, so projections are constrained by historical climatology
- Increased winter sea ice loss in CMIP6 is related to increased equilibrium climate sensitivity

Supporting Information:

Supporting Information may be found in the online version of this article.

Correspondence to:

C. R. Holmes,
calmes@bas.ac.uk

Citation:

Holmes, C. R., Bracegirdle, T. J., & Holland, P. R. (2022). Antarctic sea ice projections constrained by historical ice cover and future global temperature change. *Geophysical Research Letters*, *49*, e2021GL097413. https://doi.org/10.1029/2021GL097413

Received 8 FEB 2022
Accepted 23 APR 2022

Abstract There is low confidence in projections of Antarctic sea ice area (SIA), due to deficiencies in climate model sea ice processes. Ensemble regression techniques can help to reduce this uncertainty. We investigate relationships between SIA climatology and 21st century change in the Coupled Model Intercomparison Project, phase 6 (CMIP6) multi-model ensemble. In summer, under a strong forcing scenario, each model loses the majority of its sea ice. Therefore, models with greater historical SIA exhibit greater reductions, so the observed climatology of SIA strongly constrains projections. Ensemble spread in historical summer SIA is smaller than in CMIP phase 5 (CMIP5), and CMIP6 gives a more robust constraint on future SIA. In winter, by 2100 under a strong forcing scenario, 40% of SIA disappears on average, and ensemble spread in historical mean SIA explains approximately half the spread in projected change. A greater winter ice loss in CMIP6 than CMIP5 is explained by the higher climate sensitivities of some CMIP6 models.

Plain Language Summary Antarctic sea ice area is important for ecosystems, human activity, and for the dynamics of the atmosphere and ocean. However, major climate change assessments such as the Intergovernmental Panel on Climate Change Sixth Assessment Report have placed little confidence in projections of Antarctic sea ice area. This is because climate models struggle to simulate many aspects of sea ice area as observed by satellites. However, not all models should be treated equally. Models with relatively more sea ice area in the recent past project greater losses in the future, especially in summer. This suggests that models with historical sea ice area closest to what we have observed may be more reliable in their future simulations. We use this information in a simple statistical model to show that, firstly, the newest climate models largely show near-total sea ice loss in summer by the end of the 21st century, which was not universally true for older climate models. Secondly, newer climate models lose more winter sea ice than their predecessors in the same time period, which is related to the known greater global warming response to given greenhouse gas concentrations in the newer models.

1. Introduction

Antarctic sea ice is a key constituent of the regional and global climate system. Its seasonal formation, transport and melt constrain the density structure of the Southern Ocean (e.g., Haumann et al., 2016), affecting heat uptake and storage (Haumann et al., 2020), and imposing a critical control on the global ocean circulation (Abernathey et al., 2016; Pellichero et al., 2018). Regionally, sea ice moderates coastal climate, while its variability and trends are key drivers of temperature fluctuations especially on the western Antarctic Peninsula (Turner et al., 2020). Projected changes in sea surface conditions have a dominant role in future projections of surface climate across the continent (Krinner et al., 2014), and therefore in the surface mass balance. Locally, future sea ice change will be critical for ecosystems (e.g., Cavanagh et al., 2017; Trathan et al., 2020) and have implications for human activities in the Southern Ocean.

Coupled climate models are our main tools for making centennial-scale projections of the climate system, but often have large biases in their representations of Antarctic sea ice and the Southern Ocean. Two recent studies (Roach et al., 2020; Shu et al., 2020) have assessed the skill of the Coupled Model Intercomparison Project, phase 6 (CMIP6) (Eyring et al., 2016) in simulating Antarctic sea ice. Both conclude that it is not obvious whether CMIP6 is an improvement over the previous generation, CMIP, phase 5 (CMIP5) (Taylor et al., 2012). There has been a reduction in inter-model spread in time-mean sea ice cover across seasons, but the multi-model mean bias in summer (February) has increased in CMIP6. Moreover, both studies show that the majority of contributing models simulate negative trends when run under historical forcing (Roach et al., 2020), while observed trends have been weakly positive (Parkinson, 2019).

The most recent Intergovernmental Panel on Climate Change (IPCC) assessment report, AR6, has not included projections of Antarctic sea ice loss in their headline statements due to "low confidence in projections". Specifically, they attribute this to "deficiencies of process representation" (Fox-Kemper et al., 2021). Holmes et al. (2019) found that a few models do capture processes driving the winter evolution of sea ice, suggesting that model selection could provide an avenue for reliable projections in this field.

While improvement in process representation will be necessary to improve confidence in projections, we can assess and reduce the uncertainty in existing projections by analyzing mean-state biases. In previous multi-model ensembles, there is a relationship between the historical state and future response of Antarctic sea ice extent (SIE; e.g., Bracegirdle et al., 2015); models with a greater SIE climatology in the recent past lose more ice in the future. This suggests that an emergent constraint, where the observed value of historical sea ice cover is combined with the multi-model relationship, may allow a constrained projection. Such constraints are an active research area in climate science, and IPCC AR6 used them as part of projections of future global mean surface temperature (Lee et al., 2021). Emergent relationships found in multi-model ensembles may have no physical basis, and therefore may not operate in the real world. However, in the case of sea ice cover, a "capacity for change" argument (Kajtar et al., 2021) partly explains the relationship; a model cannot simulate the loss of sea ice that is not present to begin with. Therefore, regardless of simulation of processes or trends, an accurate simulation of climatological mean sea ice cover is a necessary condition for accurate projections.

In the Arctic, coupled climate models also simulate a wide range of historical biases (Notz & Community, 2020) and do not in general capture the magnitude of recent trends (e.g., Rosenblum & Eisenman, 2017). Nevertheless, motivated by sudden observed declines in 2007 and 2012 and greater direct human interaction with the northern sea ice zone, considerable effort has gone into predicting metrics of sea ice behavior such as the "ice-free date" (e.g., Notz & Community, 2020).

In this paper, we present projections of Antarctic sea ice area (SIA) in CMIP6. Our main purpose is to establish whether relationships between SIA historical climatology and its future change seen in past multimodel ensembles remain in CMIP6, and whether CMIP6 gives us any greater confidence in projections. First, we revisit the results of Roach et al. (2020) and Shu et al. (2020), and highlight a specific improvement in CMIP6 versus CMIP5, namely the eradication of summer high-biased models. We also quantify future change in the full ensemble. Secondly, we analyze relationships between historical SIA and future SIA change for February and September separately. Thirdly, driven by evidence of increased SIA loss in CMIP6, we probe the relationships between SIA change and global temperature change.

2. Data and Methods

This paper analyses SIA. This is calculated as gridded sea ice concentration (expressed as a fraction) multiplied by grid cell area, integrated around Antarctica. Observational uncertainty in SIA is greater than that in SIE. However, SIE is highly dependent on grid scale (Notz, 2014). Therefore, SIA is more robust for multi-model intercomparisons, or model-observation comparisons, and our use of SIA follows other CMIP6 analyses (Notz & Community, 2020; Roach et al., 2020).

The additional observational uncertainty introduced by using SIA is important if making projections that incorporate observations, such as in an emergent constraint. We use satellite remote sensing data from two algorithms; NASA-Team v1.1 (Cavalieri et al., 1996) and Bootstrap v3.1 (Comiso, 2017). NASA-Team SIA is lower throughout the year and especially in winter (e.g., Figure S2 in Supporting Information S1). SIA is analyzed in February ("summer") and September ("winter"), the months of climatological minimum and maximum SIA in observations.

For specifics on the CMIP5 and CMIP6 sea ice variables used, see Text S1 in Supporting Information S1. We also calculate model annual-mean global mean surface air temperature, from CMIP variable *tas*.

We use the *historical* experiment, and focus on projections from "strong" forcing experiments- CMIP5 rcp85 (Meinshausen et al., 2011) and CMIP6 ScenarioMIP ssp585 (O'Neill et al., 2016). We also present results from "moderate" (rcp45, ssp245) and "weak" (rcp26, ssp126) scenario runs. Historical means are calculated for the period 1979–2014 to make use of the maximum satellite period overlapping with the CMIP6 historical

Table 1
CMIP5 and CMIP6 Ensemble Projected Ice Change ΔSIA_F (M km^2) for Differing Values of Radiative Mean Forcing, F (W m^{-2})

				Multi-model ensemble SIA projections			
Generation	Forcing F	Month	n	Min	Mean	Max	Range
CMIP5	2.6	February	24	−1.24	−0.28	0.53	1.78
CMIP6	2.6	February	25	−1.77	−0.43	0.38	2.15
CMIP5	4.5	February	33	−1.9	−0.52	0.12	2.02
CMIP6	4.5	February	27	−1.9	−0.65	0.07	1.97
CMIP5	8.5	February	34	−3.91	−1.09	−0.02	3.90
CMIP6	8.5	February	26	−3.31	−0.95	0.00	3.31
CMIP5	2.6	September	24	−4.41	−1.31	2.49	6.90
CMIP6	2.6	September	25	−7.38	−1.82	0.69	8.08
CMIP5	4.5	September	33	−6.23	−1.96	2.60	8.83
CMIP6	4.5	September	27	−10.61	−3.19	0.16	10.77
CMIP5	8.5	September	34	−9.02	−4.32	1.27	10.30
CMIP6	8.5	September	26	−12.90	−5.71	−0.17	12.74

Note. CMIP6, Coupled Model Intercomparison Project, phase 6; SIA, sea ice area. Columns show size of the ensemble, n, and multi-model ensemble statistics in February and September.

simulations. For CMIP5, historical runs ended in 2005; data for years to 2014 is taken from rcp45 or, where this is unavailable, rcp85. End-of-the-century climatologies are defined following the IPCC standard (2081–2100).

We use notation $\boldsymbol{SIA_{hist}}$ for historical SIA climatology, and $\Delta\boldsymbol{SIA_F}$ for the difference between the future and historical values under the scenario with radiative forcing F (e.g., $\Delta\boldsymbol{SIA_{8.5}}$ for change under scenarios rcp85 and ssp585, which have radiative forcing 8.5Wm^{-2}). Similarly, the change in global mean surface temperature is denoted $\Delta\boldsymbol{TAS_F}$. We also use "equilibrium climate sensitivity' (ECS) from Meehl et al. (2020); see Text S1 for details and discussion.

To produce constrained projections we use a linear regression model obtained from regressing $\Delta\boldsymbol{SIA}_{8.5}$ against $\boldsymbol{SIA_{hist}}$ to predict future change, using one of the observational datasets as the predictor. Linear regression analysis uses python's statsmodels ordinary least squares method.

All individual model metrics and regression statistics are given in Holmes (2022) [dataset].

3. Results

3.1. Projected SIA Change in CMIP6

For both CMIP5 and CMIP6, the multi-model mean projection is for SIA loss in all forcing scenarios, for both summer and winter, by the end of the 21st century (Table 1). Under all scenarios except the strongest forcing (rcp85 and ssp585), there is at least one model, in both seasons and both CMIP5 and CMIP6, which simulates SIA increase by the end of the century. Roach et al. (2020) concluded that the historical simulation of SIA in CMIP6 was not notably improved, if at all, over CMIP5. Table 1 shows that, furthermore, the uncertainty in September projections as quantified by the inter-model range is greater in CMIP6 than CMIP5. There also appears to be some change in sensitivity to forcing in September; multi-model mean $\Delta\boldsymbol{SIA_F}$ is consistently of greater magnitude in CMIP6 than in CMIP5. In February, the direction of CMIP5 to CMIP6 change in inter-model range is scenario-dependent, as is the change in multi-model mean $\Delta\boldsymbol{SIA_F}$. To investigate these apparent differences between the ensembles, and examine their potential importance for SIA projections, we investigate the relationship between $\boldsymbol{SIA_{hist}}$ and $\Delta\boldsymbol{SIA_F}$.

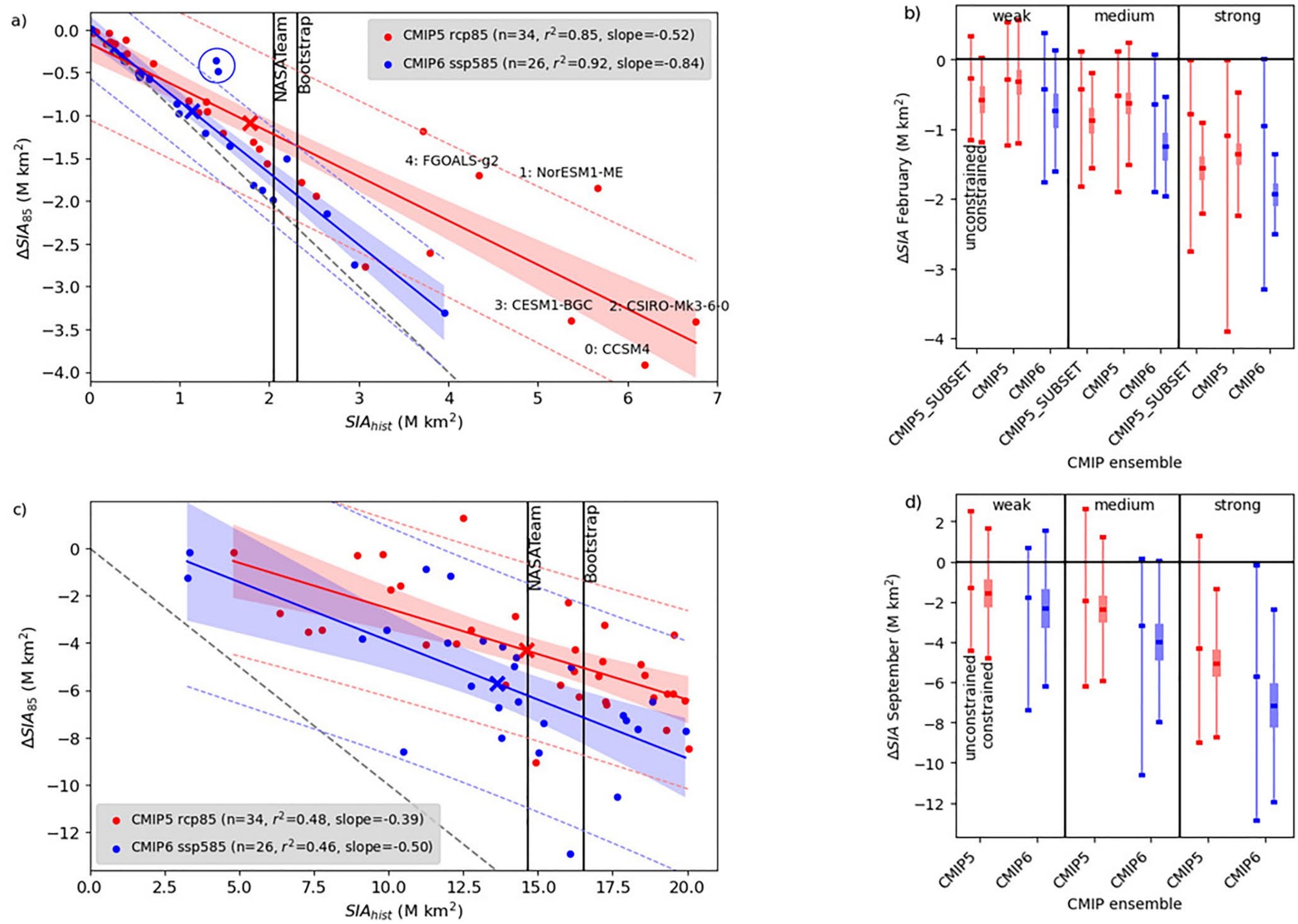

Figure 1. The emergent relationship between $\boldsymbol{SIA_{hist}}$ and $\Delta\boldsymbol{SIA_F}$, and its consequences for projections, for CMIP5 (red) and CMIP6 (blue). (a) February $\Delta\boldsymbol{SIA_{8.5}}$ versus February $\boldsymbol{SIA_{hist}}$. Thick solid colored lines indicate the linear regression model; shading indicates the confidence interval; the dashed line indicates the prediction interval. Observations are indicated in black; the multimodel mean by a cross; and the one-to-one line by a gray dashed line. Circled points are NorESM2 models. (b) Projections from the unconstrained and constrained ensembles, for "weak", "medium" and "strong" forcing scenarios (see Data and Methods). For each ensemble (x-axis tick), the first set of points shows the minimum, mean and maximum $\boldsymbol{SIA_F}$ from the unconstrained ensemble. The second set of points shows the mean projection, its 5%–95% confidence interval (shaded rectangle), and the 5%–95% uncertainty range on the prediction, using the ensemble constraint and Bootstrap observations. (c) as (a) but for September. (d) as (b) but for September, and with no CMIP5_subset.

3.2. Emergent Relationship in February (Summer)

3.2.1. CMIP6

In CMIP6 (Figure 1a) there is a strong linear relationship ($r^2 = 0.92$) between $\boldsymbol{SIA_{hist}}$ and $\Delta\boldsymbol{SIA_{8.5}}$. Many of the points lie almost on the one-to-one-line (gray dashed line, Figure 1a), indicating that models lose most of their ice by the end of the century in this scenario. Therefore, this statistical relationship has a mechanistic explanation arising from a practical limit on ice loss. This is analogous to the “capacity for change” argument of Kajtar et al. (2021), although they discuss other aspects of the Southern Ocean climate system (not only sea ice) and consider the annual mean, therefore not reaching the limit of zero sea ice.

Strictly, the "physical limit" argument applies only to models which lose all their ice. We therefore introduce a conceptual distinction between "Group 1: All ice lost" models and "Group 2: Some ice retained" models. Group 1 is defined as models whose SIA drops below a threshold of 0.1 Mkm^2 by the end of the 21st century (Text S2 and Figure S3b in Supporting Information S1). For these models, the correlation between $\boldsymbol{SIA_{hist}}$ and $\Delta\boldsymbol{SIA}$ is very high and constrained by the one-to-one line. These models dominate in CMIP6 (20/26), leading to the strong correlation for the full ensemble. Furthermore, within Group 1, models with smaller $\boldsymbol{SIA_{hist}}$ lose their ice sooner; this suggests that historical climatology could have predictive power for the time of ice loss as well as its magnitude (Text S2 in Supporting Information S1).

For "Group 2" models, a different, weaker relationship holds between $\boldsymbol{SIA}_{hist}$ and $\Delta\boldsymbol{SIA}$ (Text S2 in Supporting Information S1). "Group 2" models dominate in the "weak" ($r^2 = 0.34$, $p < 0.01$) and "moderate" forcing scenarios ($r^2 = 0.71$, $p < 0.01$) (Figure S1 in Supporting Information S1).

An understanding of the mechanism for this emergent relationship, due to the dominance of "Group 1" models, provides a basis for using it to make predictions about the future state of the real world (Data and Methods, final paragraph). We discuss our confidence in this interpretation in the Discussion section. The resulting constrained prediction for $\Delta\boldsymbol{SIA}_{8.5}$ in CMIP6 is for greater ice loss than predicted by the multimodel mean (Figure 1b). The constraint also gives a narrower uncertainty range, which does not encompass near-zero ice loss. The existence of a narrowed uncertainty range is robust to using $\mu \pm 2\boldsymbol{\sigma}$ (where μ and $\boldsymbol{\sigma}$ are the ensemble mean and standard deviation) rather than maximum and minimum as a quantification of ensemble spread. We display maximum and minimum because the ensemble distribution of $\Delta\boldsymbol{SIA}_F$ is heavily skewed. Using NASA-Team observations to constrain the projection would imply weaker ice loss than shown in Figure 1b), but still greater than the multimodel mean.

Two models, NorESM2-LM and NorESM2-MM, which lose much less ice in all forcing scenarios than implied by the linear regression (Figure 1a, circled), are discussed in Text S3 of Supporting Information S1.

3.2.2. Comparison to CMIP5

The relationship between climatology and future change is weaker for CMIP5 (Figure 1a, red). This is due to a smaller proportion of "Group 1" models in CMIP5 (12/34); and in particular due to CMIP5 models with large positive $\boldsymbol{SIA}_{hist}$ biases, which retain a lot of ice. There are no such highly-biased models in the CMIP6 ensemble. This change represents an improvement in the ensemble representation of Antarctic sea ice, although it results in an increase in the magnitude of the multi-model mean negative bias (Roach et al., 2020).

We wish to test the hypothesis that the relationships in CMIP5 and CMIP6 are consistent over their shared historical range; that is, that the difference in $\Delta\boldsymbol{SIA}_{8.5}$ between the ensembles is due only to the change in $\boldsymbol{SIA}_{hist}$. We therefore create the reduced ensemble "CMIP5_subset", consisting of only CMIP5 models whose $\boldsymbol{SIA}_{hist}$ falls within the CMIP6 historical range (0.01–3.95 Mkm^2). The excluded models are labeled in Figure 1b) and discussed in Text S3 in Supporting Information S1.

The regression slope in CMIP5_subset is more strongly negative than that in CMIP5 as a whole (Figure S3a in Supporting Information S1), although the relationship does not explain any more of the variance. The regression slope is more strongly negative in CMIP6 than in either CMIP5 or CMIP5_subset, leading to a constrained prediction of greater ice loss in CMIP6 (Figure 1b). Outliers within the shared historical range may be strongly influencing this difference; therefore, there is weak evidence that sea ice in CMIP6 models is more sensitive to a strong greenhouse gas forcing scenario than in CMIP5 models. "Time of ice loss" analysis (Figure S3b in Supporting Information S1) supports this evidence, since it suggests that for a given $\boldsymbol{SIA}_{hist}$, CMIP6 models are more likely to have lost all ice by 2100 than CMIP5 models. Comparing the ensemble means alone (e.g., Table 1) would give the opposite conclusion about the relative sea ice sensitivity of the model ensembles.

The individual projections of the high-biased CMIP5 models are not possible in reality, because some predict the loss of more ice than is currently observed. Furthermore, our results suggest that a linear regression is not a helpful descriptor of the CMIP5 ensemble, due to the greater dominance of "Group 2" models and in particular high-biased models which do not lie close to the one-to-one line (Figure 1a) and thus alter the linear regression (compare Figure S3a in Supporting Information S1 with Figure 1a). We do not assess the realism of this nonlinear behavior for high $\boldsymbol{SIA}_{hist}$, because observations lie in the range where a linear regression does appear to be a good description of the relationship between climatology and change. Therefore, we conclude that CMIP6 has a more consistent projection of total ice loss under a strong forcing scenario, and the improvement in the underlying ensemble gives us confidence in this change.

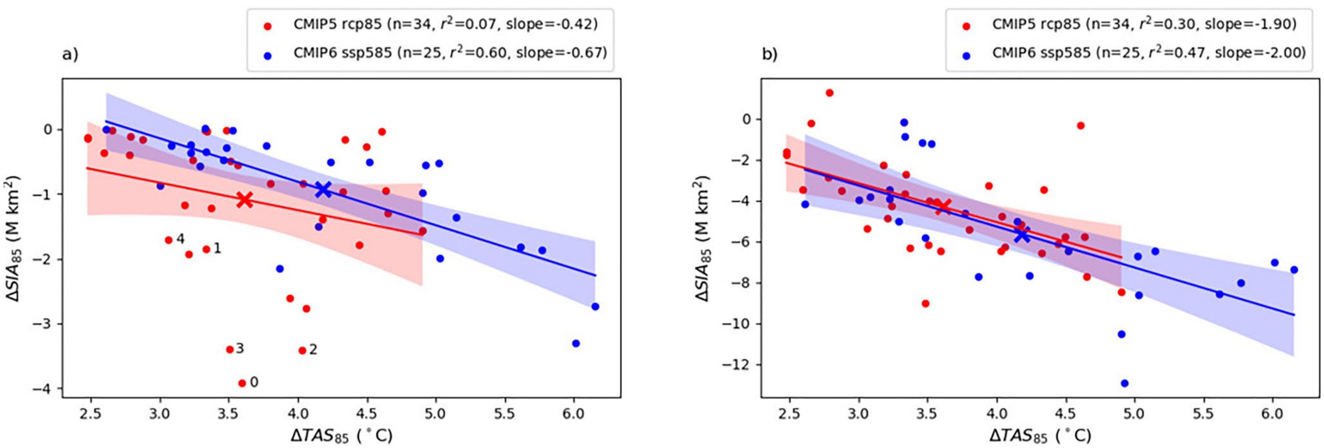

Figure 2. Relationship of global mean temperature change $\Delta \boldsymbol{TAS}_{8.5}$ with sea ice change $\Delta \boldsymbol{SIA}_{8.5}$. (a) February, with CMIP5 high-climatology models from Figure 1a indicated numerically; (b) September. Note non-zero limit on x-axis. Other details as in Figure 1a.

3.3. September (Winter)

In September (Figure 1c), likewise, models with more sea ice in the historical period lose more ice. For both ensembles, this relationship is weaker than for February, but the historical climatology still explains nearly 50% of the variance in projections for the "strong" forcing scenario. The relationship is present in the "medium" forcing scenario, but in the "weak" scenario is not statistically significant or only weakly so (Holmes, 2022). Shu et al. (2020) excluded the CMIP6 MIROC models from their analysis due to extreme biases (<5 Mkm^2 winter sea ice; Figure 1c far left). Removing this pair of models does not change the regression slope, but reduces the CMIP6 variance explained to 30%.

The no-ice limit described in February does not explain this relationship. Other proposed physical mechanisms for emergent constraints include a "growth-thickness" feedback (Bitz, 2008; Bitz & Roe, 2004) whereby thick, extensive multi-year Arctic ice thins more rapidly than thin ice. However, the relevance of this for the more seasonal Antarctic ice, and for projections of area rather than volume, is unclear.

CMIP6 models lose more sea ice on average than those in CMIP5 (Figure 1c, crosses). In the range of historical values close to observations, confidence intervals on the regression (pale colored lines, Figure 1c) for CMIP5 and CMIP6 do not overlap, implying that this difference between ensembles is statistically significant. This is true despite a similar range of historical climatologies, implying that the multi-model relationship between climatology and change cannot explain the difference.

As a hypothesis to explain this difference, we turn to the fact that the upper end of ECS in CMIP6 exceeds that in CMIP5 (e.g., Zelinka et al., 2020). This quantifies the fact that global temperature in CMIP6 models responds more strongly to CO_2 forcing than in CMIP5 models on centennial timescales. We therefore explore the hypothesis that the greater SIA loss in CMIP6 is driven by greater global temperature change, by analyzing first the within-ensemble relationship between $\Delta \boldsymbol{TAS}$ and $\Delta \boldsymbol{SIA}$, and then the difference between ensembles. We conduct this analysis for both seasons for completeness.

3.4. Relationship With Global Temperature Change

3.4.1. February

Analysis of models with a shared range of $\boldsymbol{SIA}_{hist}$, and threshold exceedance analysis, provided weak evidence of greater summer sea ice sensitivity to greenhouse gas forcing in CMIP6 than CMIP5 (Figure 1b). Examining the relationship between $\Delta \boldsymbol{TAS}_{8.5}$ and $\Delta \boldsymbol{SIA}_{8.5}$ for CMIP6 models reveals a moderate relationship ($r^2 = 0.60$; Figure 2a, blue). Excluding the four strongest warming models, r^2 falls to 0.28 and the slope weakens to −0.41 (not shown; see data), suggesting the relationship is dominated by these four models. No such relationship exists in CMIP5 (Figure 2a), and the previously discussed CMIP5_subset (excluding models with high $\boldsymbol{SIA}_{hist}$, numbered in Figure 2a as in Figure 1a) also has only a weakly significant regression. In the absence of a consistent relationship between $\Delta \boldsymbol{SIA}_{8.5}$ and $\Delta \boldsymbol{TAS}_{8.5}$ across the ensembles, we cannot confidently conclude that the greater global warming in CMIP6 is driving greater sea ice loss.

We recall that CMIP6 models lose most of their summer ice (Figure 1), giving a correlation of almost 1 between $\boldsymbol{SIA}_{hist}$ and $\Delta \boldsymbol{SIA}_{8.5}$. Therefore, the relationship between $\Delta \boldsymbol{TAS}_{8.5}$ and $\Delta \boldsymbol{SIA}_{8.5}$ (Figure 2a) implies that $\boldsymbol{SIA}_{hist}$ and $\Delta \boldsymbol{TAS}_{8.5}$ are not independent. Indeed, in CMIP6 these values are positively correlated, such that models with higher February $\boldsymbol{SIA}_{hist}$ warm more ($r^2 = 0.45$; not shown). This relationship exists in all CMIP6 forcing scenarios, but not CMIP5. Kajtar et al. (2021) found that, while models with a colder midlatitude Southern Ocean in CMIP5 have greater global warming, this relationship between local baseline temperature and global temperature change shifts to the sea ice zone in CMIP6. This therefore appears consistent with the existence of a relationship between summer $\boldsymbol{SIA}_{hist}$ and $\Delta \boldsymbol{TAS}_{8.5}$ in CMIP6, as found here (Figure 2a). An investigation of the mechanisms behind this relationship is beyond the scope of the paper. One hypothesis, that models that warm more in the 21st century have already warmed more and therefore lost more ice in the historical period, would have led to the opposite relationship.

3.4.2. September

Global temperature change explains 47% of the variance in projections of CMIP6 September ice loss (Figure 2b). In contrast to February, this relationship is also statistically significant, although weaker, in CMIP5. The modest relationship in CMIP5 is slightly stronger than the relationship ($r = -0.4$, $r^2 = 0.16$) between CMIP5 annual mean Antarctic $\Delta \boldsymbol{SIA}_{8.5}$ and global $\Delta \boldsymbol{TAS}_{8.5}$ found in Bracegirdle et al. (2015); our model subset differs, but results are partially reconciled ($r^2 = 0.21$) if we use annual mean $\Delta \boldsymbol{SIA}_{8.5}$.

The regression slope is statistically indistinguishable for the two ensembles. However, CMIP6 models warm more on average (Figure 2b, crosses), so that this same slope corresponds to the greater ice loss found in CMIP6. Similar results apply for weaker forcing scenarios (Figure S4 in Supporting Information S1). We therefore conclude that greater winter SIA loss in CMIP6 is related to the greater global warming. Warming in the 21st century under a strong forcing scenario and ECS are highly correlated (e.g., Grose et al., 2018), and indeed, correlations between ECS and $\Delta \boldsymbol{SIA}_{8.5}$ are similar to correlations between $\Delta \boldsymbol{TAS}_{8.5}$ and $\Delta \boldsymbol{SIA}_{8.5}$ (not shown).

Finally, given the relationships found for September between $\Delta \boldsymbol{SIA}$ and both $\boldsymbol{SIA}_{hist}$ and $\Delta \boldsymbol{TAS}$, we perform a multiple regression to quantify their combined role in explaining ensemble spread in projections. This regression has $r^2 = 0.65$ for CMIP6 $\Delta \boldsymbol{SIA}_{8.5}$ ($r^2 = 0.40$ for $\Delta \boldsymbol{SIA}_{4.5}$ and $r^2 = 0.35$ for $\Delta \boldsymbol{SIA}_{2.6}$).

4. Conclusions and Discussion

In this study, we have for the first time presented an overview of CMIP6 projections for 21st century Antarctic SIA change, $\Delta \boldsymbol{SIA}$. In the light of large ensemble spread (uncertainty), and lack of confidence in model projections, we have examined two drivers of ensemble spread in $\Delta \boldsymbol{SIA}$ and their importance in different seasons, and the scope for constraining projections based on model-observation comparisons of the past.

In CMIP6 (as in CMIP5; Bracegirdle et al., 2015), $\boldsymbol{SIA}_{hist}$ is strongly related to $\Delta \boldsymbol{SIA}$ (an emergent relationship), especially under a strong forcing scenario in February (summer). Here, a "capacity for change" argument provides a physical basis for using this emergent relationship to observationally constrain model projections of $\Delta \boldsymbol{SIA}$. The constrained CMIP6-based projection shows a clear loss of all summer sea ice by the end of the 21st century under strong forcing. This is not the case in CMIP5. There is also stronger loss in CMIP6 than CMIP5 for projections based on other forcing scenarios. A prominent reason for the stronger emergent constraint on CMIP6 February projections is that there are a number of models with very large positive $\boldsymbol{SIA}_{hist}$ biases in CMIP5, but not in CMIP6. The eradication of such biases is a substantial advance for climate modeling, and the more consistent relationship between climatology and change is an important consequence. Our confidence in this statistical prediction is discussed later.

There is a relationship, albeit weaker, between $\boldsymbol{SIA}_{hist}$ and $\Delta \boldsymbol{SIA}$ in September; here, the regression has similar slope and r^2 values for CMIP5 and CMIP6 but there is an offset such that CMIP6 SIA loss is greater. In all forcing scenarios, models which warm more globally in the 21st century lose more September sea ice. Further, greater sea ice loss in CMIP6 than CMIP5 is related to the presence of models with higher ECS in CMIP6.

Therefore, constraining Antarctic SIA loss under strong (or indeed moderate) forcing scenarios is related to constraining ECS. This is an ongoing topic of research. Sherwood et al. (2020) reviewed three lines of evidence - recent warming, the paleoclimate record, and feedback understanding - and concluded that both high and low extreme values of ECS were unlikely, suggesting that the high-end ECS CMIP6 climate models are unrealistic. The IPCC sixth Assessment Report confirmed this assessment (Lee et al., 2021), concluding that there was a 90% probability of the full ECS lying within the 2–5°C range. This implies that the greater SIA loss in CMIP6 found in this paper may be an artifact of this too-high ECS and warming in CMIP6. Southern Ocean cloud processes, particularly mixed-phase cloud feedbacks, have been an emerging theme in understanding of the higher ECS in CMIP6 (e.g., Zelinka et al., 2020; Bjordal et al., 2020). Since cloud cover is important for sea ice, this could imply a more complex interaction than sea ice merely responding to warming.

Having discussed the plausibility of the global temperature response to forcing (the x-axis in Figure 2), we now address our confidence in the relationship between SIA change and that warming. Implicitly, this will also inform our confidence in the projection of total summer ice loss.

It is possible that all or most climate models have SIA that is too sensitive to global temperature changes. A first line of evidence is based on a historical mismatch between observed positive SIA trends and simulated negative SIA trends. Specifically, CMIP models that capture near-to-observed historical sea ice trends have too little global warming (equivalently models with realistic warming have too-negative sea ice trends; Rosenblum & Eisenman, 2017). This result also holds in CMIP6 (Roach et al., 2020, Figure 3). Even models with tropical variability nudged to observations, a proposed mechanism driving discrepancy between observed and modeled sea ice trends, do not capture historical sea ice trends, implying the forced sea ice response is too strong (Schneider & Deser, 2018). The implications for model projections on centennial timescales under strong forcing is unclear. However, sensitivity experiments based on physical arguments suggest that this result may hold; standard CMIP experiment protocols do not incorporate ongoing increases in freshwater flux from Antarctic ice sheets. Including such fluxes has been shown to mitigate sea ice loss over the 21st century in coupled models with a range of historical states (compare Bronselaer et al., 2018; Bintanja et al., 2015; Sadai et al., 2020). Further, Rackow et al. (2022) demonstrates that a climate model with a high resolution, locally eddy-resolving, ocean component simulates slower sea-ice decline than its standard resolution counterpart; this implies that standard resolution models have too-fast decline.

In summary, we show evidence to support the assertion that when evaluating sea ice projections from a model ensemble a key step is to exploit emergent relationships between historical climatology and response to extract a more precise ensemble mean projection. However, it is also clear that potential systematic ensemble-wide biases and/or missing processes in aspects such as global climate sensitivity and freshwater input from ice sheets are key to assessing accuracy in projections.

Data Availability Statement

CMIP data can be accessed through the ESGF data portals (see http://pcmdi-cmip.llnl.gov/cmip5/availability.html and esgf-node.llnl.gov/search/cmip6). Individual model details and metrics calculated for this paper, and all ensemble regression statistics, are available at the Polar Data Centre via [https://doi.org/10.5285/e67242f2-e9aa-4402-85a3-be42d13354af] (Holmes, 2022).

Acknowledgments

The authors were funded by the Natural Environment Research Council as part of the British Antarctic Survey Polar Science for Planet Earth Programme and grant NE/N01829X/1. The World Climate Research Programme's Working Group on Coupled Modelling, which is responsible for CMIP, and the climate modeling groups, are thanked for producing and making available their model output.

References

Abernathey, R. P., Cerovecki, I., Holland, P. R., Newsom, E., Mazloff, M., & Talley, L. D. (2016). Water-mass transformation by sea ice in the upper branch of the Southern Ocean overturning. *Nature Geoscience*, *9*(8), 596–601. https://doi.org/10.1038/ngeo2749

Bintanja, R., Van Oldenborgh, G., & Katsman, C. (2015). The effect of increased fresh water from Antarctic ice shelves on future trends in Antarctic sea ice. *Annals of Glaciology*, *56*(69), 120–126. https://doi.org/10.3189/2015AoG69A001

Bitz, C. M. (2008). Some aspects of uncertainty in predicting sea ice thinning. *Arctic Sea Ice Decline: Observations, Projections, Mechanisms, and Implications, Geophys. Monogr*, *180*, 63–76. https://doi.org/10.1029/180gm06

Bitz, C. M., & Roe, G. H. (2004). A mechanism for the high rate of sea ice thinning in the Arctic Ocean. *Journal of Climate*, *17*(18), 3623–3632. https://doi.org/10.1175/1520-0442(2004)017<3623:amfthr>2.0.co;2

Bjordal, J., Storelvmo, T., Alterskjær, K., & Carlsen, T. (2020). Equilibrium climate sensitivity above 5 C plausible due to state-dependent cloud feedback. *Nature Geoscience*, *13*(11), 718–721. https://doi.org/10.1038/s41561-020-00649-1

Bracegirdle, T. J., Stephenson, D. B., Turner, J., & Phillips, T. (2015). The importance of sea ice area biases in 21st century multimodel projections of Antarctic temperature and precipitation. *Geophysical Research Letters*, *42*(24), 10–832. https://doi.org/10.1002/2015GL067055

Bronselaer, B., Winton, M., Griffies, S. M., Hurlin, W. J., Rodgers, K. B., Sergienko, O. V., et al. (2018). Change in future climate due to Antarctic meltwater. *Nature*, *564*(7734), 53–58. https://doi.org/10.1038/s41586-018-0712-z

Cavalieri, D. J., Parkinson, C. L., Gloersen, P., & Zwally, H. J. (1996). Sea Ice Concentrations from Nimbus-7 SMMR and DMSP SSM/I-SSMIS Passive Microwave Data, Version 1.1. [Dataset]. NASA National Snow and Ice Data Center Distributed Active Archive Center. [Accessed Apr 1 2021], updated yearly. https://doi.org/10.5067/8GQ8LZQVL0VL

Cavanagh, R. D., Murphy, E. J., Bracegirdle, T. J., Turner, J., Knowland, C. A., Corney, S. P., et al. (2017). A synergistic approach for evaluating climate model output for ecological applications. *Frontiers in Marine Science*, *4*, 308. https://doi.org/10.3389/fmars.2017.00308

Comiso, J. C. (2017). Bootstrap Sea Ice Concentrations from Nimbus-7 SMMR and DMSP SSM/I-SSMIS, Version 3.1. [Dataset]. NASA National Snow and Ice Data Center Distributed Active Archive Center. [Accessed Apr 1 2021]. https://doi.org/10.5067/7Q8HCCWS4I0R

Eyring, V., Bony, S., Meehl, G. A., Senior, C. A., Stevens, B., Stouffer, R. J., & Taylor, K. E. (2016). Overview of the Coupled Model Intercomparison Project Phase 6 (CMIP6) experimental design and organization. *Geoscientific Model Development*, *9*(5), 1937–1958. https://doi.org/10.5194/gmd-9-1937-2016

Fox-Kemper, B., Hewitt, H. T., Xiao, C., Aðalgeirsdóttir, G., Drijfhout, S. S., Edwards, T. L., et al. (2021). Ocean, cryosphere and sea level change. In V. Masson-Delmotte, P. Zhai, A. Pirani, S. L. Connors, C. Péan, S. Berger, et al. (Eds.), *Climate change 2021: The physical science basis. Contribution of working group I to the sixth assessment report of the intergovernmental panel on climate change* (pp. 55–56). Cambridge University Press.

Grose, M. R., Gregory, J., Colman, R., & Andrews, T. (2018). What climate sensitivity index is most useful for projections? *Geophysical Research Letters*, *45*(3), 1559–1566. https://doi.org/10.1002/2017GL075742

Haumann, F. A., Gruber, N., & Münnich, M. (2020). Sea-ice induced Southern Ocean subsurface warming and surface cooling in a warming climate. *AGU Advances*, *1*(2), e2019AV000132. https://doi.org/10.1029/2019av000132

Haumann, F. A., Gruber, N., Münnich, M., Frenger, I., & Kern, S. (2016). Sea-ice transport driving Southern Ocean salinity and its recent trends. *Nature*, *537*(7618), 89–92. https://doi.org/10.1038/nature19101

Holmes, C. (2022). Sea Ice Area climatologies and 21st century change in the CMIP5 and CMIP6 multi-model ensembles (Version 1.0) [Data set]. NERC EDS UK Polar Data Centre. https://doi.org/10.5285/E67242F2-E9AA-4402-85A3-BE42D13354AF

Kajtar, J. B., Santoso, A., Collins, M., Taschetto, A. S., England, M. H., & Frankcombe, L. M. (2021). CMIP5 intermodel relationships in the baseline Southern Ocean climate system and with future projections. *Earth's Future*, *9*(6), e2020EF001873. https://doi.org/10.1029/2020EF001873

Krinner, G., Largeron, C., Ménégoz, M., Agosta, C., & Brutel-Vuilmet, C. (2014). Oceanic forcing of Antarctic climate change: A study using a stretched-grid atmospheric general circulation model. *Journal of Climate*, *27*(15), 5786–5800. https://doi.org/10.1175/JCLI-D-13-00367.1

Lee, J. Y., Marotzke, J., Bala, G., Cao, L., Corti, S., Dunne, J. P., et al. (2021). Future global climate: Scenario-based projections and near-term information. In V. Masson-Delmotte, P. Zhai, A. Pirani, S. L. Connors, C. Péan, S. Berger, et al. (Eds.), *Climate change 2021: The physical science basis. Contribution of working group I to the sixth assessment report of the intergovernmental panel on climate change* (pp. 55–56). Cambridge University Press.

Meehl, G. A., Senior, C. A., Eyring, V., Flato, G., Lamarque, J. F., Stouffer, R. J., et al. (2020). Context for interpreting equilibrium climate sensitivity and transient climate response from the CMIP6 Earth system models. *Science Advances*, *6*(26). https://doi.org/10.1126/sciadv.aba1981

Meinshausen, M., Smith, S. J., Calvin, K., Daniel, J. S., Kainuma, M. L. T., Lamarque, J.-F., et al. (2011). The RCP greenhouse gas concentrations and their extensions from 1765 to 2300. *Climatic Change*, *109*(1–2), 213–241. https://doi.org/10.1007/s10584-011-0156-z

Notz, D. (2014). Sea-ice extent and its trend provide limited metrics of model performance. *The Cryosphere*, *8*(1), 229–243. https://doi.org/10.5194/tc-8-229-2014

Notz, D., & SIMIP Community. (2020). Arctic sea ice in CMIP6. *Geophysical Research Letters*, *47*(10), e2019GL086749. https://doi.org/10.1029/2019GL086749

O'Neill, B. C., Tebaldi, C., Vuuren, D. P. V., Eyring, V., Friedlingstein, P., Hurtt, G., et al. (2016). The scenario model intercomparison project (ScenarioMIP) for CMIP6. *Geoscientific Model Development*, *9*(9), 3461–3482. https://doi.org/10.5194/gmd-9-3461-2016

Parkinson, C. L. (2019). A 40-y record reveals gradual Antarctic sea ice increases followed by decreases at rates far exceeding the rates seen in the Arctic. *Proceedings of the National Academy of Sciences of the United States of America*, *116*(29), 14414–14423. https://doi.org/10.1073/pnas.1906556116

Pellichero, V., Sallée, J. B., Chapman, C. C., & Downes, S. M. (2018). The southern ocean meridional overturning in the sea-ice sector is driven by freshwater fluxes. *Nature Communications*, *9*(1), 1–9. https://www.nature.com/articles/s41467-018-04101-2

Rackow, T., Danilov, S., Goessling, H. F., Hellmer, H. H., Sein, D. V., Semmler, T., et al. (2022). Delayed Antarctic sea-ice decline in high-resolution climate change simulations. *Nature Communications*, *13*(637). https://doi.org/10.1038/s41467-022-28259-y

Roach, L. A., Dörr, J., Holmes, C. R., Massonnet, F., Blockley, E. W., Notz, D., et al. (2020). Antarctic sea ice area in CMIP6. *Geophysical Research Letters*, *47*(9), e2019GL086729. https://doi.org/10.1029/2019GL086729

Rosenblum, E., & Eisenman, I. (2017). Sea ice trends in climate models only accurate in runs with biased global warming. *Journal of Climate*, *30*(16), 6265–6278. https://doi.org/10.1175/JCLI-D-16-0455.1

Sadai, S., Condron, A., DeConto, R., & Pollard, D. (2020). Future climate response to Antarctic Ice Sheet melt caused by anthropogenic warming. *Science Advances*, *6*(39), eaaz1169. https://doi.org/10.1126/sciadv.aaz1169

Schneider, D. P., & Deser, C. (2018). Tropically driven and externally forced patterns of Antarctic sea ice change: Reconciling observed and modeled trends. *Climate Dynamics*, *50*(11), 4599–4618. https://doi.org/10.1007/s00382-017-3893-5

Sherwood, S. C., Webb, M. J., Annan, J. D., Armour, K. C., Forster, P. M., Hargreaves, J. C., et al. (2020). An assessment of Earth's climate sensitivity using multiple lines of evidence. *Reviews of Geophysics*, *58*(4), e2019RG000678. https://doi.org/10.1029/2019RG000678

Shu, Q., Wang, Q., Song, Z., Qiao, F., Zhao, J., Chu, M., & Li, X. (2020). Assessment of sea ice extent in CMIP6 with comparison to observations and CMIP5. *Geophysical Research Letters*, *47*(9), e2020GL087965. https://doi.org/10.1029/2020GL087965

Taylor, K. E., Stouffer, R. J., & Meehl, G. A. (2012). An overview of CMIP5 and the experiment design. *Bulletin of the American Meteorological Society*, *93*(4), 485–498. https://doi.org/10.1175/BAMS-D-11-00094.1

Trathan, P. N., Wienecke, B., Barbraud, C., Jenouvrier, S., Kooyman, G., Le Bohec, C., et al. (2020). The emperor penguin- Vulnerable to projected rates of warming and sea ice loss. *Biological Conservation*, *241*, 108216. https://doi.org/10.1016/j.biocon.2019.108216

Turner, J., Marshall, G. J., Clem, K., Colwell, S., Phillips, T., & Lu, H. (2020). Antarctic temperature variability and change from station data. *International Journal of Climatology*, *40*(6), 2986–3007. https://doi.org/10.1002/joc.6378

Zelinka, M. D., Myers, T. A., McCoy, D. T., Po-Chedley, S., Caldwell, P. M., Ceppi, P., et al. (2020). Causes of higher climate sensitivity in CMIP6 models. *Geophysical Research Letters*, *47*(1), e2019GL085782. https://doi.org/10.1029/2019gl085782

References From the Supporting Information

Gregory, J. M., Ingram, W. J., Palmer, M. A., Jones, G. S., Stott, P. A., Thorpe, R. B., et al. (2004). A new method for diagnosing radiative forcing and climate sensitivity. *Geophysical Research Letters*, *31*(3), L03205. https://doi.org/10.1029/2003GL018747

Gjermundsen, A., Nummelin, A., Olivié, D., Bentsen, M., Seland, Ø., & Schulz, M. (2021). Shutdown of Southern Ocean convection controls long-term greenhouse gas-induced warming. *Nature Geoscience*, *14*(10), 724–731. https://doi.org/10.1038/s41561-021-00825-x

Holmes, C. R., Holland, P. R., & Bracegirdle, T. J. (2019). Compensating biases and a noteworthy success in the CMIP5 representation of Antarctic sea ice processes. *Geophysical Research Letters*, *46*(8), 4299–4307. https://doi.org/10.1029/2018GL081796